

The effect of high magnetic field on phase stability in Fe-Ni

D. M. C. Nicholson,^{a)} R. A. Kisner, G. M. Ludtka, C. J. Sparks, L. Petit, Roger Jaramillo, G. Mackiewicz-Ludtka, and J. B. Wilgen
Oak Ridge National Laboratory, Department of Computer Science and Mathematics,
MS6164 Building 5700, One Bethel Valley Road, Oak Ridge, Tennessee 37831

Askar Sheikh-Ali and P. N. Kalu

FAMU-FSU, National High Magnetic Field Laboratory, Tallahassee, FL 32310

(Presented on 6 January 2004)

Identically prepared samples of $\text{Fe}_{0.85}\text{Ni}_{0.15}$ were annealed either in the ambient magnetic field or in a field of 29 T. Room temperature x-ray powder diffraction measurements that were performed after magnetic annealing showed that the ratio of the volume of the γ to α phase is decreased in the field-annealed sample by a factor of 2. First-principles calculations of the magnetic structure in the presence of a magnetic field are used to compute the resulting change in free energy. Analysis in terms of the phase diagram calculated with and without a magnetic field is in substantial agreement with the measurements. © 2004 American Institute of Physics. [DOI: 10.1063/1.1689761]

In this article, we emphasize that applied magnetic field should be added to the list of thermodynamic variables, and we give an example where the application of a magnetic field leads to a new temperature composition path. Previous work on the application of high fields to Ni-Fe is reviewed by Shimizu and Kakeshita.¹ In addition, small fields have been used to anneal soft magnetic materials to produce subtle modifications in the local atomic environment that can increase the permeability.² A simple perturbative estimate of the energy change due to the interaction of the atomic moments with the field, $\mathbf{m}\cdot\mathbf{B}$, indicates that a 1 T field changes the free energy per atom in Fe by about the same amount as changing the temperature by 1 K. By the same token, when applying the highest available fields, 30–40 T is expected to have impacts similar to temperature changes of 30–40 K.

There are several ways that magnetic fields can influence microstructure. Most directly, it can change the relative stability of phases at zero temperature. Consider a two-phase mixture with different saturation magnetizations. The magnetic induction \mathbf{B} will favor the high magnetization phase by an amount $(\mathbf{m}_{\text{high}} - \mathbf{m}_{\text{low}})\cdot\mathbf{B}$, where \mathbf{m} is the atomic moment. At finite temperatures there can be additional mechanisms; thermally occupied extended excitations, such as spin waves and phonons, and localized excitations, such as vacancy facilitated diffusion, will be affected.

Fe alloys are a natural place to look for field-induced modifications of phase equilibrium, because Fe atoms have large local moments that have strong exchange interactions with their neighbors. Local Fe moments survive to high temperatures and to large percentages of alloy additions.^{3,4} Furthermore, the directional ordering of Fe moments can vary from ferromagnetic to antiferromagnetic depending on the atomic volume.⁵ We chose to look at Fe-Ni alloys at compositions in the two-phase region between the bcc and fcc solid solutions (α and γ phases). The temperature was chosen to be 500 °C, a temperature at which diffusion is expected to be

high enough to allow equilibrium to be approached within a few hours. The selected composition was $\text{Fe}_{85}\text{Ni}_{15}$, which lies on the T_0 line along which the free energies of the α and γ phases are equal.⁶ This is also near the Martensite start temperature.⁷ Placing the alloy at this balance point maximizes the local driving force toward phase separation (see Fig. 1). The sample should phase separately even without diffusion into bcc and fcc solid solutions. Phase fractions will proceed toward the value prescribed by the lever rule as shown in Fig. 1. We anticipated that the application of a large magnetic field would tip the balance in favor of the ferromagnetic bcc phase.

An alloy of atomic composition $\text{Fe}_{0.85}\text{Ni}_{0.15}$, prepared from Ni and Fe stock of 0.999% purity, was arc melted in a vacuum five times, and then dropcast into a 10 mm diameter chilled Cu mold in vacuum. The alloy was homogenized in a vacuum for 100 h at 1100 °C. A small amount of powder was made by diamond wheel grinding and then encapsulated in 10 mm diameter stainless steel tubes that were crimped and sealed by electron discharge machining. All powder capsules were annealed together at 700 °C for 2 h to obtain the equilibrium γ phase, and were quenched in ice salt brine. A powder sample was subjected to a 29 T field for 245 min at

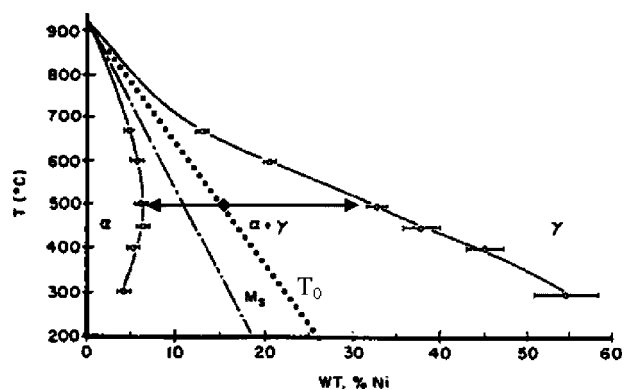


FIG. 1. Fe-rich section of phase diagram showing martensite start temperature, equal free energy line, and decomposition path at 500 °C (Ref. 8).

^{a)} Author to whom correspondence should be addressed; electronic mail: nicholsondm@ornl.gov

TABLE I. Peak intensities divided by peak multiplicity for the α peaks for anneal with ($B=29$ T) and without field ($B=0$ T).

hkl	110	200	211
$P/m(B=0)$	1.000	0.468	0.256
$P/m(B=29)$	1.000	0.419	0.268
F^2	313	267	178
$\sin(\theta)/\lambda$	0.25	0.35	0.43

502 °C. As a control, one of the identically prepared samples was annealed for 245 min at 502 °C in the ambient field. The samples were rapidly heated from room temperature to 502 °C. They were air cooled at a rate of 100 °C/min. The field-annealed sample remained in the field until it had cooled 85 °C, at which time the field was turned off.

The volume fractions of the α and γ phases were determined using $\text{CuK}\alpha$ radiation from a Philips diffractometer. Several diamond peaks resulting from diamond wheel grinding were seen. The diamond peaks are sufficiently separated from the Fe-Ni peaks that they do not interfere with measurements of the integrated intensities.

In the kinematic approximation to diffraction, and with the use of a compensating slit, the integrated intensity associated with a particular reflection hkl is related to the volume fraction V_i of phase i and the scattering angle 2θ by⁹

$$P_{hkl,i} = \frac{I_0}{16\pi R} \frac{e^4 V_i m_{hkl} F_i^2}{m^2 c^4 \Omega_i^2} \left(\frac{1 + \cos^2(2\theta)}{2 \sin^2(\theta)} \right) E \left(\frac{\sin(\theta)}{\lambda} \right). \quad (1)$$

Here, E represents absorption effects not present in an infinitely thick powder in the kinematic limit, I_0 is the beam intensity, m_{hkl} is the reflection multiplicity, R is the distance to the detector, λ is the wavelength (1.54 Å), Ω_i is the atomic volume, and F_i is the average atomic scattering factor for the phase i . The scattering factor, F_i is equal to

$$\left| c_i F_{\text{Fe}} \left(\frac{\sin(\theta)}{\lambda} \right) + (1 - c_i) F_{\text{Ni}} \left(\frac{\sin(\theta)}{\lambda} \right) \right|,$$

where c_i is the Fe concentration of phase i and F_j is the atomic scattering factor of element j . Because Fe and Ni have similar atomic numbers, their scattering factors are similar and the average scattering factor at a given θ varies by less than 10% for any concentration that can possibly occur in our samples. A further simplifying coincidence is that the scattering factor is independent of concentration near the first α and γ peaks, $\sin(\theta)/\lambda=0.24$. Therefore, when the ratio of the first two peak intensities is taken, many of the factors in Eq. (1) cancel and some factors almost cancel. For example, the atomic volumes, scattering amplitudes, and

TABLE II. Same as Table I, but for γ peaks.

hkl	111	200	220	311	222
$P/m(B=0)$	0.383	0.302	0.111	0.075	0.066
$P/m(B=29)$	0.207	0.135	0.067	0.041	0.041
F^2	312	254	172	133	122
$\sin(\theta)/\lambda$	0.24	0.28	0.39	0.43	0.46

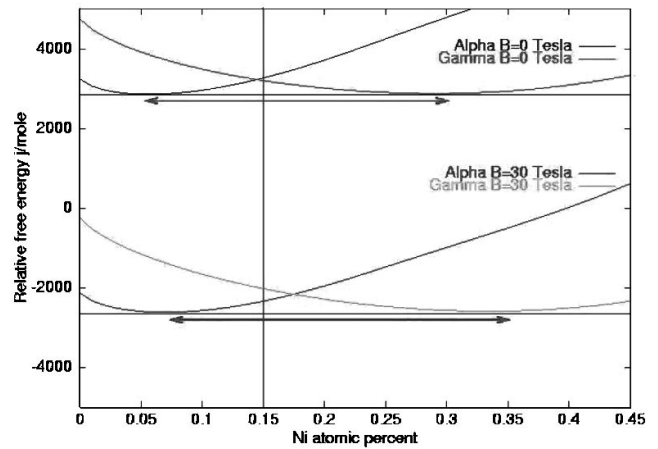


FIG. 2. Free energy with and without applied field. Arrows indicate the phase concentrations.

$\sin(\theta)/\lambda$ are almost equal. When performing these nearly exact cancellations, an extremely simple expression relating $P_{111\gamma}/P_{110\alpha}$ to the volume ratio is obtained:

$$\frac{m_{110}}{m_{111}} \frac{P_{111\gamma}}{P_{110\alpha}} = \frac{V_\gamma}{V_\alpha} = R_0. \quad (2)$$

This simple relation gives the volume fraction $F_{B=0} = V_\gamma/V_{B=0 \text{ total}} = R_{B=0}/(1 + R_{B=0})$ to within 1% of the full expression, Eq. (1).

The integrated intensities under each peak divided by the multiplicity are given in Tables I and II, along with the value of $\sin(\theta)/\lambda$ and the atomic scattering factors. The integrated intensities are in arbitrary units and have been normalized to give $P_{110}/m_{110}=1.0$ for both samples.

The simplicity of Eq. (2) allows us to read $R_{B=0}$ from the data for the 110 and 111 peaks; We find $R_{B=0}=0.383$ and $F_{B=0}=0.28$. The value of 0.28 is smaller than the equilibrium values of 0.355 ± 0.03 from application of the lever rule to the phase diagram.⁸ To put this discrepancy into perspective, consider that an uncertainty in our annealing temperature of 10 °C results in an additional uncertainty in the expected volume fraction of ± 0.01 ; an uncertainty of 1% in our alloy composition results in an additional uncertainty in the expected volume fraction of ± 0.03 . Our uncertainty in temperature and composition should be smaller than 10 °C and 1%, so our low observed γ volume fraction needs explanation. The difference between our value and the measured equilibrium phase diagram could reflect that either our system has not reached equilibrium or that the value of E in Eq. (1) is not the same for the two phases. By using data from all

TABLE III. S calculated from ratios of peak areas for different peak pairs, (area bcc)/(area fcc).

α	γ				
	111	200	220	311	222
100	1.85	2.24	1.67	1.80	1.59
200	1.65	2.00	1.49	1.60	1.42
211	1.94	2.35	1.75	1.88	1.66

peaks we can approximately account for the combined effects of thermal diffuse scattering, surface roughness, finite sample thickness, preferred orientation, and deviations from the kinematic approximation (extinction). Such an analysis gives an average value of $F_{B=0}=0.30\pm 0.03$ that is consistent with the value of 0.28 obtained from the simple formula Eq. (1) and compares reasonably to the previously measured value of 0.355 ± 0.03 from the data of Fig. 1.⁸

This result gives a baseline from which to measure the effect of the magnetic anneal. If we know the relative reduction, $S=R_{B=0}/R_{B=29}$, in R induced by the field we can determine the resulting phase fraction,

$$F_{B=29} = \frac{F_{B=0}}{S + SF_{B=0} - F_{B=0}}. \quad (3)$$

The value of S can be deduced from intensity ratios:

$$\frac{\left(\frac{P_{hkl}^\gamma}{P_{h'k'l'}^\alpha} \right)_{B=0 \text{ T}}}{\left(\frac{P_{hkl}^\gamma}{P_{h'k'l'}^\alpha} \right)_{B=29 \text{ T}}} = S \frac{\left[\frac{F^2(c_\gamma, \theta_{hkl}) E_\gamma(\theta_{hkl})}{F^2(c_\alpha, \theta_{h'k'l'}) E_\alpha(\theta_{h'k'l'})} \right]_{B=0 \text{ T}}}{\left[\frac{F^2(c_\gamma, \theta_{hkl}) E_\gamma(\theta_{hkl})}{F^2(c_\alpha, \theta_{h'k'l'}) E_\alpha(\theta_{h'k'l'})} \right]_{B=29 \text{ T}}}, \quad (4)$$

provided we have an independent determination of the atomic scattering factor and E ratios. For our sample it can be safely assumed that the scattering factor ratios cancel. We find solid evidence that E is independent of the field. Therefore the ratios reduce to 1. Table III gives S as determined from different $hkl/h'k'l'$ pairs. Averaging all the data, we obtain 1.8 ± 0.2 . The variability of S with respect to peak pairs is independent of the atomic scattering amplitude ratio but could reflect changes in E due to the field. However, the most likely source of error is the background subtraction which was done by visual interpolation of the intensity between Bragg peaks. The 222 peak has the fewest counts, and is therefore the most sensitive.

Now that S has been determined, we can use Eq. (4) by inserting the volume fraction for the sample annealed in ambient field, $F_{B=0}=0.30\pm 0.03$, to obtain the γ phase fraction of the field-annealed sample; we obtain $F_{B=29}=0.14\pm 0.03$. This demonstrates that the field reduces the amount of the γ phase by a factor of 2. The same relative reduction is obtained if the value of $F_{B=0}$ from the measured phase diagram is used in Eq. (1); the only difference being that the reduction is from 0.36 to 0.16.

For a collinear ferromagnetic material, an applied field shifts the Kohn-Sham potential of the majority electrons to lower energy. This shift results in a slight increase of the saturation magnetic moment. As the temperature is increased, ferromagnetic materials become slightly noncollinear due to thermal excitation of spin waves. Above the Curie temperature the direction of the local moments have no long range correlation and become increasingly random at higher temperatures. The locally self-consistent multiple scattering code¹⁰ was used to calculate the change in energy due to the application of a 30 T field. The additional applied magnetic field contributes a shift in the local Kohn-Sham potential along the direction of the magnetic moment and a rotation of the moment toward the direction of the field.

The thermodynamic model of Chuang *et al.*,⁶ based on experimental data, reproduces the phase diagrams in zero

field. We calculated the change in the energy resulting from the application of a magnetic field and added this contribution to the existing thermodynamic model. In this way, contributions, which we expect will not be greatly influenced by the magnetic field, such as phonon energy and entropy, can be taken from the existing model. Because we are interested in a temperature well away from the critical temperature, we can approximate the change in the partition function by summing over a small number of spin configurations. Figure 2 shows the calculated modified free energy curves for Fe-Ni at 500 °C. The α phase is found to have increased stability due to the field of 30 T. The concentration at which the α and γ curves cross is shifted to higher Ni concentration, indicating an increase in the martensite starting temperature. The field-induced change in the volume fraction of α and γ is in qualitative agreement with our measurements.

Research was sponsored by the Laboratory Directed Research and Development Program of Oak Ridge National Laboratory (ORNL), managed by UT-Battelle, LLC for the U. S. Department of Energy under Contract No. DE-AC05-00OR22725. Calculations were performed at the National Energy Research Computing Center and the Center for Computational Science, Oak Ridge National Laboratory.

¹K. Shimizu and T. Kakeshita, *ISIJ Int.* **29**, 97 (1989).

²R. M. Bozorth, *Ferromagnetism* (Van Nostrand, New York, 1951); J. C. Slonczewski, in *Magnetic Ions in Insulators: Their Interactions, Resonances, and Optical Properties*, edited by G. T. Rado (Academic, New York, 1963).

³Y. Waseda and K. Suzuki, *Phys. Status Solidi* **39**, 669 (1970).

⁴T. Hoshino, R. Zeller, and P. H. Dederichs, *J. Magn. Magn. Mater.* **140**, 113 (1995).

⁵M. Uhl *et al.*, *Phys. Rev. B* **50**, 291 (1994).

⁶Y.-Y. Chuang, Y. A. Chang, R. Schmid, and J.-C. Lin, *Metall. Mater. Trans.* **17A**, 1361 (1986).

⁷Y. E. A. Fokina, L. V. Smirnov, and V. D. Sadovsky, *Fiz. Met. Metalloved.* **27**, 756 (1969).

⁸J. Zhang, D. B. Williams, and J. I. Goldstein, *Metall. Mater. Trans. A* **25A**, 1639 (1994).

⁹B. E. Warren, *X-Ray Diffraction* (Dover, New York, 1969).

¹⁰Y. Wang *et al.*, *Phys. Rev. Lett.* **75**, 2867 (1995).